

## Electronic Supplementary Material

# Photoluminescence of CdSe Nanowires Grown With and Without Metal Catalyst

Andrea Fasoli<sup>1</sup>, Alan Colli<sup>2</sup>, Faustino Martelli<sup>3</sup>, Simone Pisana<sup>1</sup>, Ping Heng Tan<sup>4</sup>, and Andrea C. Ferrari<sup>1</sup> (✉)

<sup>1</sup> Department of Engineering, University of Cambridge, Cambridge CB3 0FA, UK

<sup>2</sup> Nokia Research Centre, Broers Building (East Forum), Cambridge CB3 0GT, UK

<sup>3</sup> Istituto per la Microelettronica e i Microsistemi del CNR, 00133 Rome, Italy

<sup>4</sup> SKLSM, Institute of Semiconductors, Chinese Academy of Sciences, Beijing 100083, China

Supporting information to DOI 10.1007/s12274-010-0089-2

### 1. Structural characterization of CdSe nanowires

The diameter distribution of Au-NWs and SG-NWs is obtained by analyzing SEM and/or TEM images of several tens of NWs (Figs. S-1(a) and S-1(b)). Au-NWs have an average diameter of  $29 \text{ nm} \pm 6 \text{ nm}$ . SG-NWs are thicker, with a broader distribution peaked at  $170 \text{ nm} \pm 80 \text{ nm}$ .

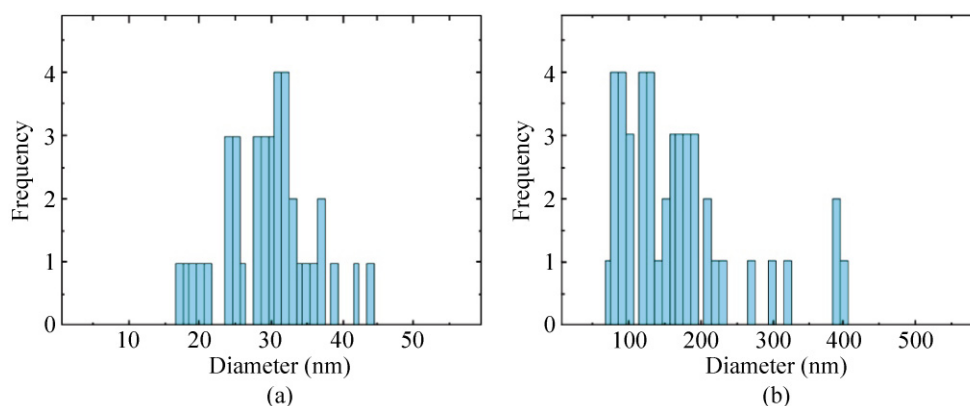


**Figure S-1** Diameter distribution of (a) Au-NWs and (b) SG-NWs

The crystal phase of Au-NWs is assessed by means of high-resolution transmission electron microscopy (HR-TEM). NWs are dispersed on a transmission electron microscopy (TEM) grid and imaged with a JEOL 4000EX-II TEM. Figure S-2(a) shows a HR-TEM lattice imaging of a representative Au-NW. The measured interplanar spacing ( $3.74 \text{ \AA}$ ) is consistent with the  $(1\bar{1}0)$  planes of a CdSe crystal with the wurtzite structure. Domains with a zinc blende structure are never observed along these NWs.

Due to their larger diameter, SG-NWs have a much lower transparency to the electron beam; As a consequence, their crystallographic structure cannot be clearly resolved by HR-TEM as in Fig. S-2(a). Instead, phase identification

Address correspondence to [acf26@eng.cam.ac.uk](mailto:acf26@eng.cam.ac.uk)



is achieved by X-ray diffraction (XRD). Figure S-2(b) shows a  $2\theta$  scan for as-grown SG-NWs on oxidized Si (inset); All peaks can be indexed to wurtzite CdSe planes, while no fingerprint of cubic CdSe is observed (the reflection from the Si substrate occurs at  $\sim 69^\circ$  and is not shown in Fig. S-2(b)). A small signal from CdO is also observed in Fig. S-2(b). A CdO layer naturally forms on the surface of CdSe NWs upon exposure to the atmosphere (similar to what observed, e.g., in Ref. [18] for ZnSe and ZnCdSe NWs).

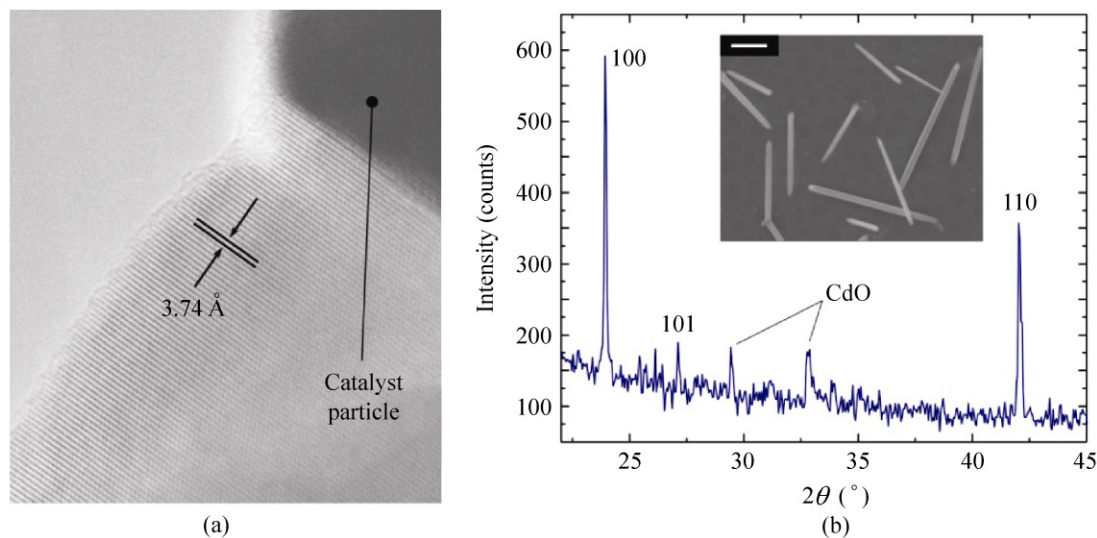


**Figure S-2** (a) HR-TEM image of a representative Au-NW; the measured lattice spacing is compatible with a CdSe crystal with the wurtzite structure. (b) XRD spectrum of as-grown SG-NWs. Peaks are indexed to wurtzite CdSe planes. Inset: SEM image of SG-NWs assessed by XRD (scale bar: 1  $\mu\text{m}$ )

The Cd/Se composition ratios of Au-NWs and SG-NWs are determined by energy dispersive X-ray (EDX) spectroscopy. Figure S-3(a) shows a SEM micrograph of an isolated Au-NW, together with the corresponding EDX analysis taken from the NW body. A near-stoichiometric Cd/Se ratio is measured, while no hint of Au is observed. The Si signal originates from the substrate. Figure S-3(b), on the other hand, shows an EDX spectrum acquired from the NW tip, where the SEM contrast of the Au catalyst particle is clearly visible. In this case, the Au EDX signal dominates over those of Cd and Se. Finally, the EDX analysis for a single SG-NW is presented in Fig. S-3(c), again showing a near-stoichiometric Cd/Se ratio as in Fig. S-3(a).

## 2. TEM mapping and characterization of individual nanowires

In order to assess the PL emission of individual Au-NWs and associate it with the corresponding TEM characterization, markers are patterned on a 50-nm-thick SiN membrane using electron beam lithography followed by Ni evaporation and lift-off. Figure S-4(a) is a low magnification TEM image of the reference membrane, showing the unique markers which are used to locate specific NWs. After patterning, Au-NWs are gently transferred by mechanical shearing from their original Si substrate to the membrane. Several high-magnification TEM micrographs are then collected to locate the NWs and characterize their morphology. Figure S-4(b) presents the overall collage of these images, which are scaled and rotated to perfectly overlap with the reference markers. The mapping reveals the location of NW bundles and isolated NWs. Both are considered to acquire sufficient statistics and to support the representative summary in Fig. 4. A NW is considered isolated (for example, spots b1, b2, and b3 in Fig. S-4) when high magnification TEM rules out the presence of additional nanostructures well beyond the size of the laser spot centered on the NW under investigation.

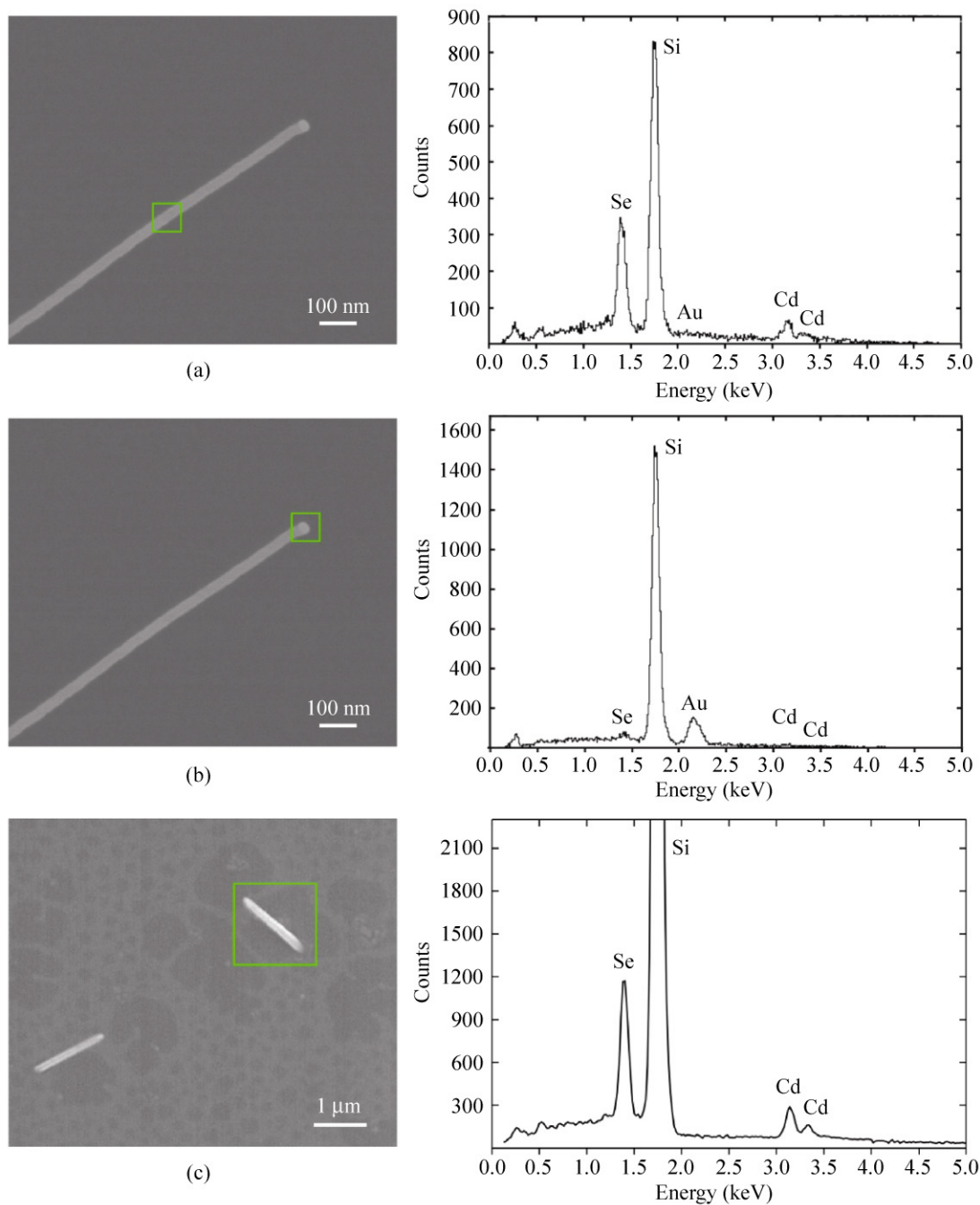


**Figure S-3** (a) SEM micrograph of an isolated Au-NW, together with (b) the corresponding EDX analysis taken from the NW body. (c) SEM micrograph of the Au-NW, together with (d) the corresponding EDX analysis taken from the NW tip. (e) SEM micrograph and (f) the corresponding EDX analysis of a SG-NW. In each case, the Cd/Se composition ratio is close to 1, once the intensities of different peaks are normalized by the appropriate cross-sections

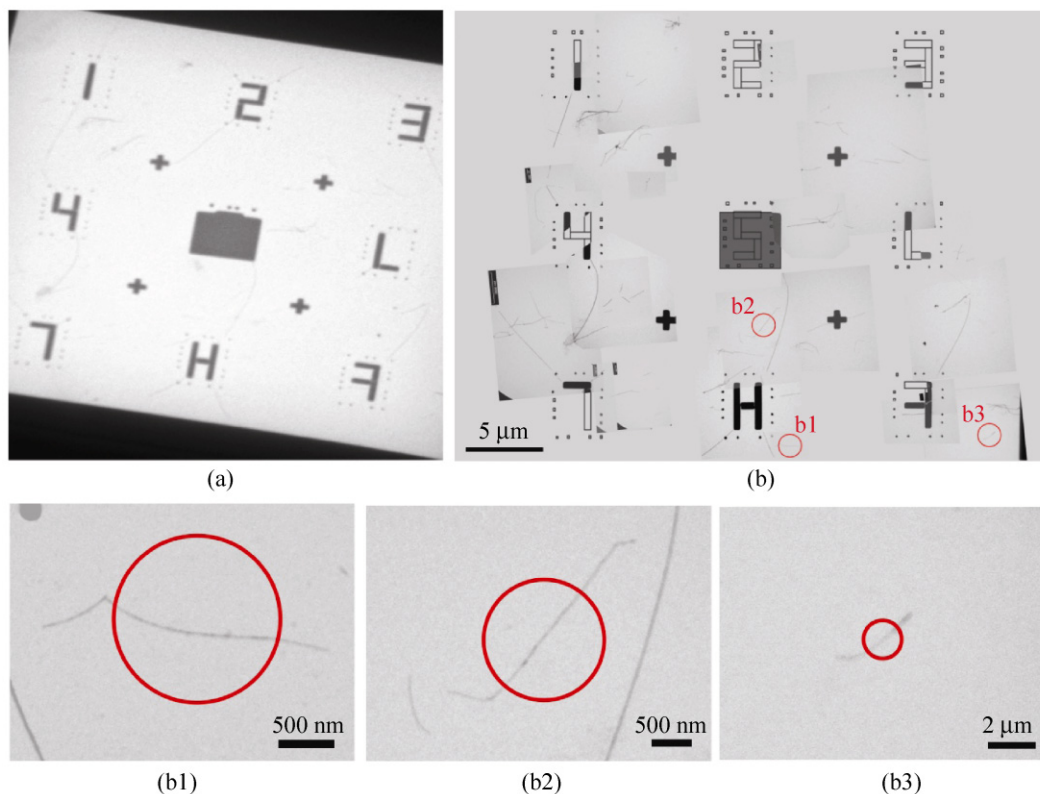


**Figure S-4** (a) Low magnification TEM image of reference markers on a SiN membrane; the black contrast surrounding the membrane is due to the Si support chip. (b) Example of NW mapping: multiple high magnification TEM images are overlapped to a scaled drawing of the pattern. Isolated NWs, (b1)–(b3), can then be located using the reference markers, and can be probed individually by the laser spot (red circles)

### 3. PL measurements before and after TEM analysis

High-dose and high-energy electron irradiation may in principle induce alterations in the NW crystal lattice. In order to rule out any effect on the PL emission due to the electron beam exposure of Au-NWs in the TEM, we compare PL spectra acquired before and after TEM imaging. Figures S-5(a) and S-5(b) show PL spectra of a NW

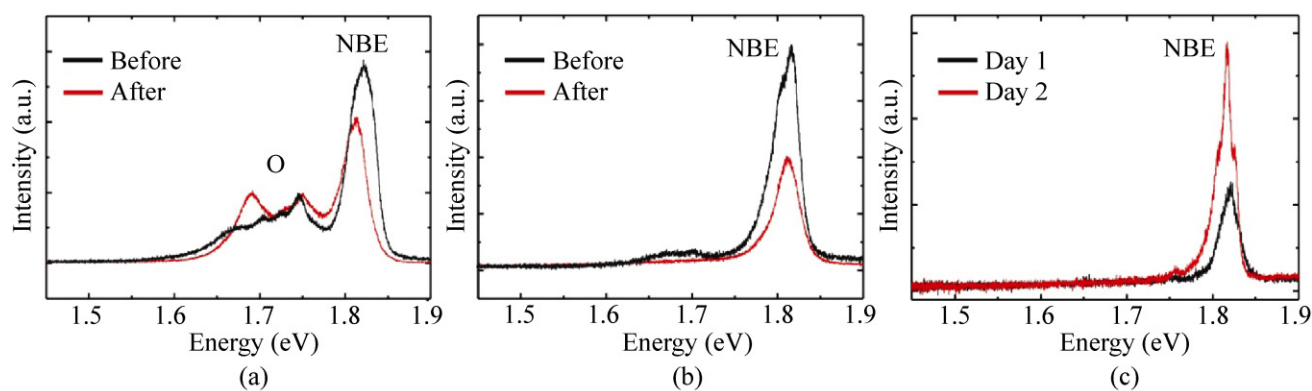


**Figure S-5** PL spectra of (a) A bundle of Au-NWs, and (b) an individual Au-NW, acquired before and after TEM imaging. (c) PL spectra of the same Au-NW acquired in different measurement sessions, showing that minor variations can occur owing to non-equivalent repositioning of the laser spot

bundle and of an isolated NW, respectively, acquired before and after electron beam exposure. For comparison, in Fig. S-5 we also plot two PL spectra taken from the same NW in separate measurement sessions, to emphasize the reproducibility tolerance arising from non-equivalent repositioning of the laser spot on the same NW after the sample has been taken off and replaced on the cryostat. These variations are not observed if the sample position is kept fixed during consecutive acquisitions using the same parameters.

It is evident that electron beam irradiation does not cause variations in PL intensity larger than the repositioning tolerance. Moreover, Fig. S-5 demonstrates that e-beam irradiation does not eliminate the O-band in NW bundles (Fig. S-5(a)), and at the same time it does not generate O-band emission in individual NWs (Fig. S-5(b)). Hence, we can consider PL spectra recorded after TEM measurements to be representative of the original NW emission.

